



# Physical CHEMISTRY

*An Indian Journal*

**Full Paper**

PCAIJ, 10(1), 2015 [12-18]

## Urbach and dispersion parameters characterization of NiO doped Fe<sub>2</sub>O<sub>3</sub> thin films

Sami Salmann Chiad

Department of Physics, College of Education, Al-Mustansiriyah University, Baghdad, (IRAQ)

### ABSTRACT

Nickel oxide doped Fe<sub>2</sub>O<sub>3</sub> thin films have been prepared by spray pyrolysis technique on glass substrate temperature 400 °C. The initial solution was including a 0.1 M/L for both NiCl<sub>2</sub> and FeCl<sub>3</sub> diluted with redistilled water and a few drops of HCl. The effect of NiO-doping on Urbach energy and dispersion parameters was studied. UV-Visible spectrophotometer in the range of (300-900) nm used to determine absorption spectra. The Urbach energy decreased with increasing NiO content that inversely proportion to the energy gap, which increased from 2.53 eV before doping to 2.88 eV after 3% NiO-doping, also the same behavior of absorbance and the optical conductivity. While the real and imaginary dielectric constants and dispersion parameters such as E<sub>d</sub>, E<sub>∞</sub>, M<sub>-1</sub>, and M<sub>-3</sub> are decreased with increasing NiO content in Fe<sub>2</sub>O<sub>3</sub> thin films.

© 2015 Trade Science Inc. - INDIA

### KEYWORDS

Fe<sub>2</sub>O<sub>3</sub>;  
NiO;  
Urbach energy;  
Dispersion Parameters.

### INTRODUCTION

Iron (III) oxide (Fe<sub>2</sub>O<sub>3</sub>) is a low-cost semiconductor having high stability and can absorb most of the visible light in the solar spectrum. Iron (III) oxide has a band gap of 2.0 to 2.2 eV; therefore, it can absorb solar radiation from 565 to 295 nm, which comprises 38% of the photons of sunlight at AM 1.5<sup>[1]</sup>. As one of the main fields of solar energy research concern the development of so-called solar fuels<sup>[2]</sup>, and considerable attention has been focused on developing new semiconductors for the photoelectron chemical (PEC) conversion<sup>[3-4]</sup>. Other applications of Fe<sub>2</sub>O<sub>3</sub> such as: catalyst<sup>[5]</sup>, a magnetic material<sup>[6]</sup>, a photo catalyst<sup>[7]</sup>, an anode in Li-ion batteries<sup>[8]</sup>, in photo electrochemical solar cells<sup>[9-</sup>

<sup>10]</sup>, a water splitter<sup>[11]</sup>, in non-linear optics<sup>[12]</sup>, and for gas sensors<sup>[13-14]</sup>.

Many researchers have worked on different techniques such as, sputtering<sup>[15]</sup>, and thermal oxidation<sup>[16]</sup>, ultrasonic spray pyrolysis (USP) and conventional spray pyrolysis (SP)<sup>[17-18]</sup>, atmospheric pressure chemical vapor deposition (APCVD) method<sup>[19]</sup>, DC reactive magnetron sputtering<sup>[20]</sup>, sol-gel method<sup>[21]</sup>, potentiostatic anodization<sup>[22]</sup>, as well as sintered disks<sup>[23]</sup> and single crystals<sup>[24-25]</sup>, for fabricating α- Fe<sub>2</sub>O<sub>3</sub> photoanodes.

Present work is to study the effect of NiO content (0, 1, and 3%) on Urbach energy and dispersion parameters of NiO:Fe<sub>2</sub>O<sub>3</sub> thin films that prepared by chemical spray pyrolysis method.

## EXPERIMENTAL

Thin films of  $\text{Fe}_2\text{O}_3$  doped by various ratios of NiO have been prepared by chemical pyrolysis technique, this technique is widely used for the large-scale production of films owing to its low production cost and simplicity of operation. A laboratory designed glass atomizer was used for spraying the aqueous solution, which has an output nozzle about 1 mm. The films were deposited on preheated cleaned glass substrates at a temperature of  $400^\circ\text{C}$ . A 0.1 M for both  $\text{NiCl}_2$  (Sigma Aldrich UK) and  $\text{FeCl}_3$  (Merck Chemicals Germany) diluted with re-distilled water and a few drops of HCl. Volumetric concentration of 1% and 3% was achieved the optimized conditions have been arriving at the following conditions; spray time was 10 s and the spray interval 2min was kept constant, the carrier gas (filtered compressed air) was maintained at a pressure of  $10^5\text{Nm}^{-2}$ , and distance between nozzle and the substrate was about  $30\text{ cm} \pm 1\text{ cm}$ .

Thickness of the sample was measured using the weighting method and was found to be around 400 nm. Optical transmittance and absorbance were recorded in the wavelength range (300-900nm) using UV-Visible spectrophotometer (Shimadzu Company Japan).

## RESULTS AND DISCUSSIONS

The absorption spectrum of  $\text{NiO}:\text{Fe}_2\text{O}_3$  thin films

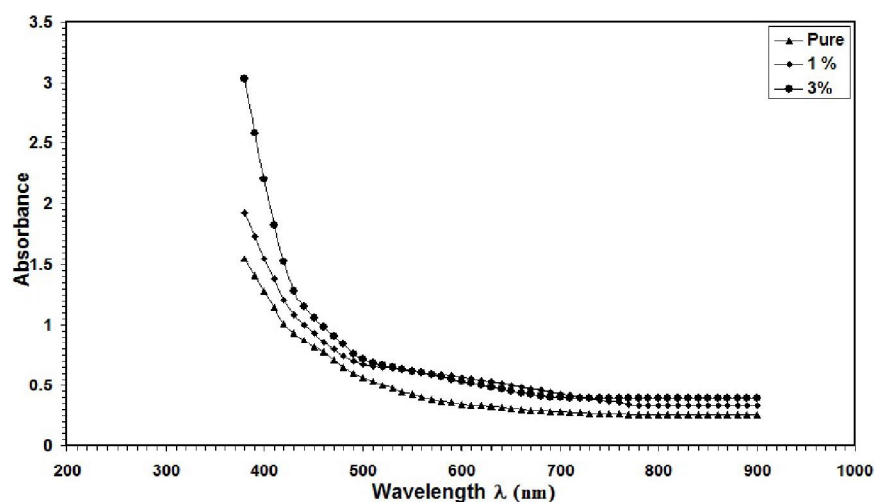


Figure 1 : The variation of optical absorbance spectra with wavelength for  $\text{NiO}:\text{Fe}_2\text{O}_3$  thin films for deferent contain of NiO

in the spectral range of (300-900) nm was prepared at substrate temperature of  $400^\circ\text{C}$  and different NiO contain is shown in Figure 1. From this figure, it can show that the spectral characterization is affected by contain of NiO. This result attributed to the creation of levels at the energy band gap, and this leads to the shift of peaks to longer wavelengths. The optical absorption spectrum decreases as the wavelength extends toward the visible region. The absorbance decreases significantly and from (600-900) nm becomes linear.

The real part ( $\epsilon_1$ ) is associated with the term that how much it will slow down the speed of light in the material and the imaginary part ( $\epsilon_2$ ) gives that how a dielectric absorb energy from electric field due to dipole motion. The real and imaginary parts of dielectric constant can be related by the following formulas<sup>[26]</sup>:

$$\epsilon_1 = n^2 - k^2 \quad (1)$$

$$\epsilon_2 = 2nk \quad (2)$$

Where  $n$  is the refractive index and  $k$  is the extinction coefficient. Figure 2 and Figure 3 are representing the relationship between  $\epsilon_1$  and  $\epsilon_2$  with wavelength. From these figures, it can notice the decreases of  $\epsilon_1$  and  $\epsilon_2$  with increasing NiO contain in  $\text{NiO}:\text{Fe}_2\text{O}_3$  thin films. This decreases more clearly in  $\epsilon_1$  than that of  $\epsilon_2$ .

The absorption coefficient ( $\alpha$ ) can be used to calculate the optical conductivity as follows<sup>[27]</sup>:

$$Q_{\text{opt}} = \frac{\alpha nc}{4\pi} \quad (3)$$

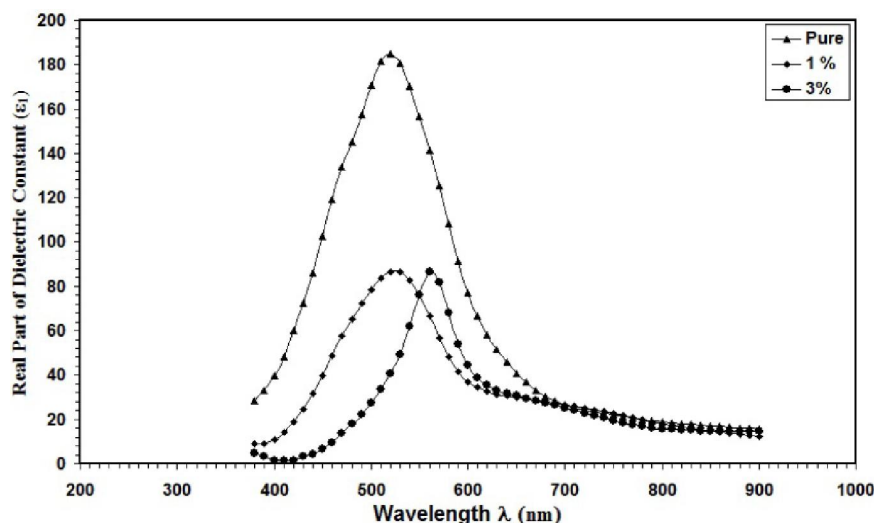


Figure 2 : The variation of real part of dielectric constant with wavelength for NiO:Fe<sub>2</sub>O<sub>3</sub> thin films for different content of NiO

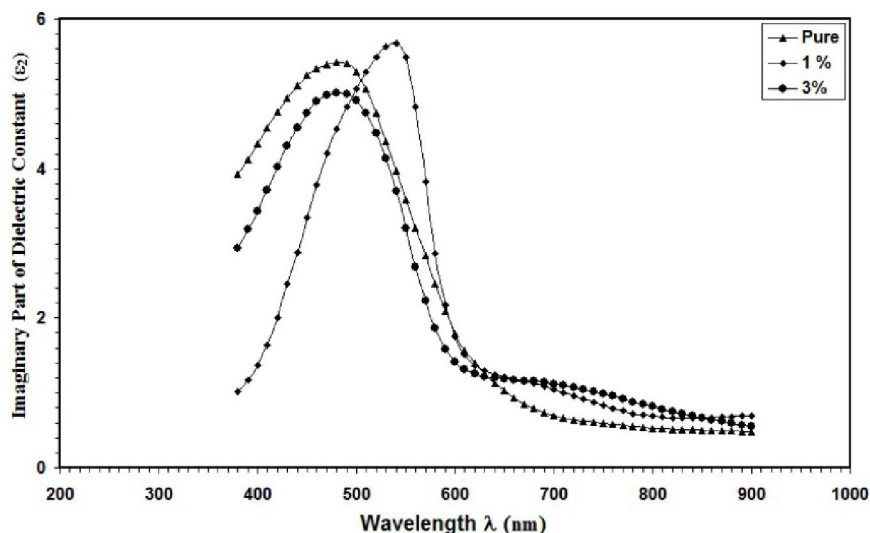


Figure 3 : The variation of imaginary part of dielectric constant with wavelength For NiO:Fe<sub>2</sub>O<sub>3</sub> thin films for different content of NiO

Where  $c$  is the velocity of light,  $n$  is the refractive index, and  $\alpha$  is the extinction coefficient. Figure 4 shows the variation of optical conductivity with wavelength. The increased of optical conductivity at low wavelengths is due to the high absorbance of NiO:Fe<sub>2</sub>O<sub>3</sub> thin films with different doping and also may be due to the electron excited by photon energy<sup>[28]</sup>.

The absorption coefficient near the band edge shows an exponential dependence on photon energy<sup>[29]</sup>:

$$\alpha(\lambda) = \alpha_0 \exp\left[\frac{h\nu}{E_U}\right] \quad (4)$$

Where  $E_U$  is the Urbach energy which corresponds to the width of the band tail and can be evaluated as

the width of the localized states,  $\alpha_0$  is a constant, and  $h\nu$  is the photon energy. Thus, a plot of  $\ln[\alpha(\lambda)]$  versus  $h\nu$  should be linear and Urbach energy can be obtained from the slope that shown in Figure 5. The Urbach energy values are listed in TABLE 1.

Wemple and DiDomenico<sup>[30-31]</sup>, used a single oscillator dispersion of the frequency-dependent dielectric constant to define “dispersion energy” parameters  $E_d$  and  $E_o$ . The dispersion plays an important role in the research for optical materials, because it is a significant factor in optical communication and in designing devices for spectral dispersion<sup>[32]</sup>. The model describes the dielectric response for transitions below the optical gap. The disper-

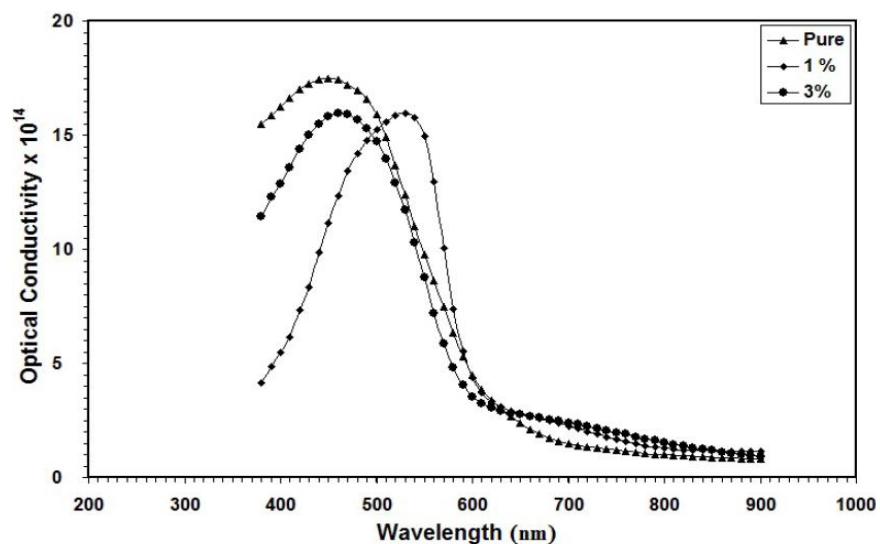


Figure 4 : The variation of optical conductivity with wavelength for NiO:Fe<sub>2</sub>O<sub>3</sub> thin films for different contain of NiO

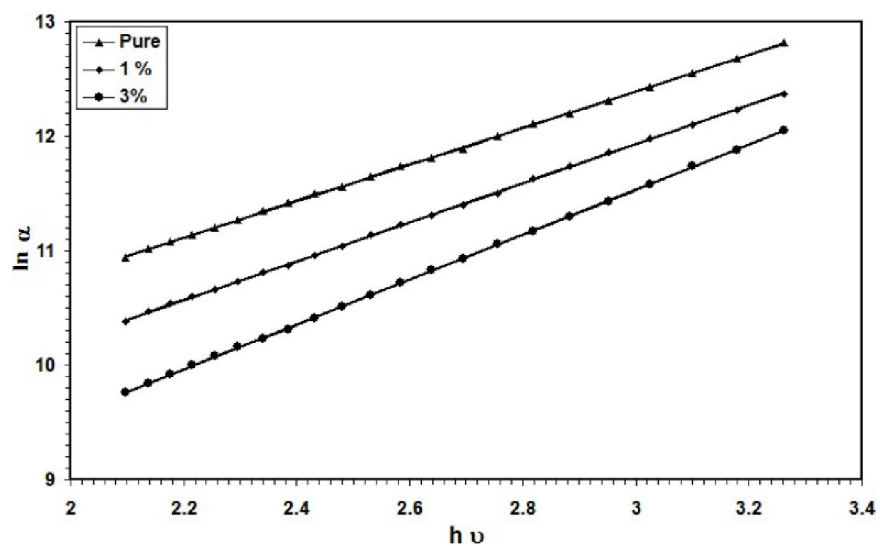


Figure 5 : The variation of  $\ln \alpha$  with photon energy for NiO:Fe<sub>2</sub>O<sub>3</sub> thin films for different contain of NiO

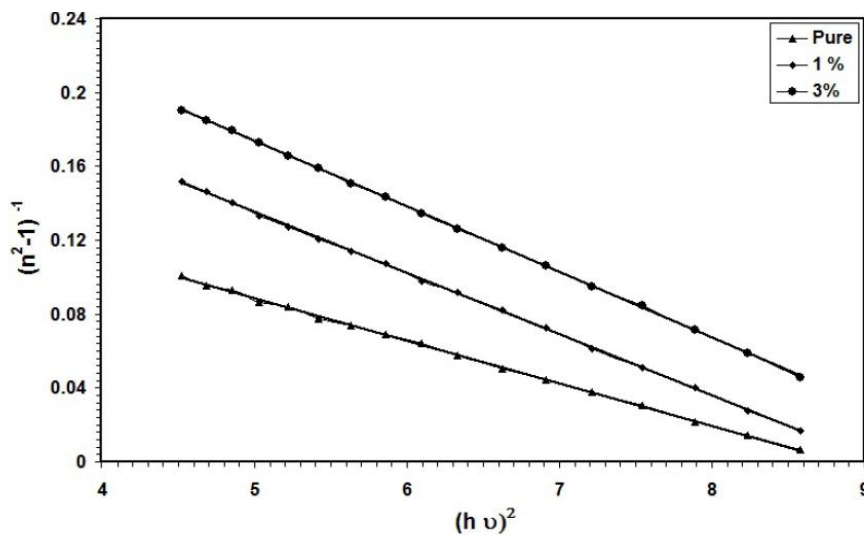


Figure 6 : The variation of  $(n^2-1)^{-1}$  with  $(h\nu)^2$  for NiO:Fe<sub>2</sub>O<sub>3</sub> thin films for different contain of NiO

## Full Paper

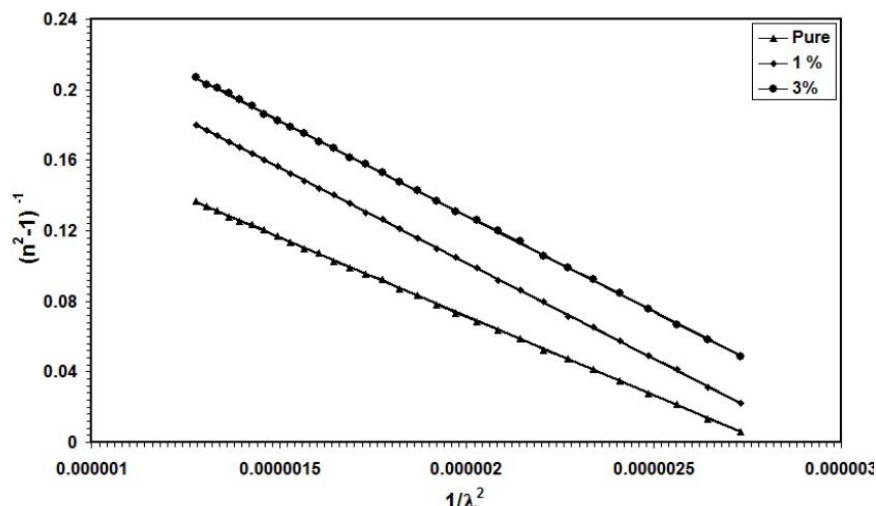


Figure 7 : The variation of  $(n^2-1)^{-1}$  with  $(1/\lambda^2)$  for NiO:Fe<sub>2</sub>O<sub>3</sub> thin films for different contain of NiO

TABLE 1 : The optical parameters of NiO:Fe<sub>2</sub>O<sub>3</sub> thin films for different content of NiO

Sample	E <sub>d</sub> (eV)	E <sub>o</sub> (eV)	E <sub>g</sub> (eV)	ε <sub>∞</sub>	n(o)	M <sub>-1</sub>	M <sub>-3</sub> (eV <sup>-2</sup> )	S <sub>o</sub> x10 <sup>13</sup> (m <sup>-2</sup> )	λ <sub>o</sub> (nm)	U <sub>E</sub> (meV)
Pure	50.64	5.06	2.53	11.00	3.32	10.00	0.39	3.35	445	625
1%	33.40	5.34	2.67	7.25	3.69	6.25	0.22	2.77	435	588
3%	28.80	5.77	2.88	6.00	2.45	5.00	0.15	2.76	404	515

sion parameters of the films were determined from the relation given by<sup>[33]</sup>:

$$n^2 = 1 + \frac{E_o E_d}{E_o^2 - E^2} \quad (5)$$

Where E<sub>o</sub> is the single oscillator energy and E<sub>d</sub> is the dispersion energy, which is a measure of the intensity of the inter band optical transitions. This model describes the dielectric response for transitions below the optical gap.  $(n^2-1)^{-1}$  vs.  $(h\nu)^2$  plots for the NiO:Fe<sub>2</sub>O<sub>3</sub> thin films was plotted (see Figure 6). E<sub>o</sub> and E<sub>d</sub> values were determined from the slope,  $(E_o E_d)^{-1}$  and intercept  $(E_o/E_d)$ , on the vertical axis. The parameter E<sub>o</sub> is an average energy gap and can be related by an empirical formula to the optical band gap value: E<sub>o</sub> = 2E<sub>g</sub><sup>[34]</sup>. The values of E<sub>o</sub>, E<sub>d</sub>, and E<sub>g</sub> are listed in TABLE 1.

The refractive index (n<sub>∞</sub>) at infinite wavelength (λ<sub>o</sub>) can be determined by the following relation<sup>[35]</sup>:

$$\frac{n_\infty^2 - 1}{n^2 - 1} = 1 - \left( \frac{\lambda_o}{\lambda} \right)^2 \quad (6)$$

The plot of  $(n^2-1)^{-1}$  vs.  $\lambda^{-2}$  was plotted to obtain n<sub>∞</sub> value of NiO:Fe<sub>2</sub>O<sub>3</sub> thin film as shown in Figure 7. The moments of the optical spectra M<sub>-1</sub> and M<sub>-3</sub> can be obtained from the relationships<sup>[36]</sup>:

$$E_o^2 = \frac{M_{-1}}{M_{-3}} \quad (7)$$

$$E_d^2 = \frac{M_{-1}^3}{M_{-3}} \quad (8)$$

The obtained M<sub>-1</sub> and M<sub>-3</sub> moments decreases with the increasing NiO contain in NiO:Fe<sub>2</sub>O<sub>3</sub> thin films as listed in TABLE 1.

## CONCLUSION

Undoped and NiO doped Fe<sub>2</sub>O<sub>3</sub> thin films were obtained by chemical spray pyrolysis method for different NiO contents. The Urbach energy decreased with increasing NiO content that lead to increase the energy gap, which increased from 2.53 eV before doping to 2.88 eV after 3% NiO-doping, also the same behavior of absorbance and the optical conductivity. While the real and imaginary dielectric constants and dispersion parameters such as E<sub>d</sub>, E<sub>∞</sub>, M<sub>-1</sub>, and M<sub>-3</sub> are decreased with increasing NiO content in Fe<sub>2</sub>O<sub>3</sub> thin films.

## REFERENCES

- [1] C.Wehrli; Extraterrestrial Solar Spectrum,

- Physikalisch-meteorologisches observatorium+world radiation center (PMO/WRC), (1985).
- [2] Y.Younsi, M.Aider, A.Bouguelia et al.; Visible light-induced hydrogen over  $\text{CuFeO}_2$  via  $\text{S}_2\text{O}_3$  oxidation, *Solar Energy*, **78**, 574 (2005).
- [3] S.Saadi, A.Bouguelia, M.Trari; Photocatalytic hydrogen evolution over  $\text{CuCrO}_2$ , *Solar Energy*, **80**, 272 (2006).
- [4] S.Boumaza, R.Bouarab, M.Trari et al.; Hydrogen photo-evolution over the spinel  $\text{CuCr}_2\text{O}_4$ , *Energy Convers Manage*, **50**, 62 (2009).
- [5] Y.Liu, D.Sun; Effect of  $\text{CeO}_2$  doping on catalytic activity of  $\text{Fe}_2\text{O}_3/\text{Al}_2\text{O}_3$  catalyst for catalytic wet peroxide of azo dyes, *J.Hazard mater*, **143**, 448 (2007).
- [6] C.Wu, P.Yin, X.Zhu, Yang CO, Y.Xie; "Synthesis of hematite ( $\alpha\text{-Fe}_2\text{O}_3$ ) nanorods, Diameter size and shape effect on their application in magnetism, Lithium ion battery and gas sensors", *J.PhysChem B*, **110**, 17806 (2006).
- [7] M.Chirita, I.Grozescu; " $\text{Fe}_2\text{O}_3$ -nanoparticle, physical properties and their photo-chemical and photoelectrochemical application", *Chem Bull "POLITEHNICA" Univ (Timisoura)*, **54**, 1 (2009).
- [8] H.S.Ryu, J.S.Kim, Z.Guo, H.Liu, K.W.Kim, J.H.Ahn, H.J.Ahn; "Electrochemical properties of  $\text{Fe}_2\text{O}_3$  thin film fabricated by electrostatic spray deposition for lithium-ion batteries", *PhysScr T*, 139 (2010).
- [9] S.S.Shinde, R.A.Bansode, C.H.Bhosale, K.Y.Rajpure; "Physical properties of hematite  $\alpha\text{-Fe}_2\text{O}_3$  thin films: application to photo electrochemical solar cells", *J.Semicond*, **32**, 8 (2011).
- [10] B.Ahmmad, Y.Kusumoto, M.Abdulla-Al-Mamun, A.Mihata, H.Yang; "Effect of single wall nanotubes as counter electrode on laser deposited  $\text{Fe}_2\text{O}_3$  and  $\text{TiO}_2$  films solar cells", *J.Sci.Res.*, **1**, 430 (2009).
- [11] S.Shen, C.X.Kronawitter, J.Jiang, S.S.Mao, L.Guo; "Surface tuning for promoted charge transfer in hematite nanorod arrays as water-splitting photoanodes", *Nano.Res.*, **5**, 327 (2012).
- [12] H.S.Zhou, A.Mito, D.Kundu, I.Honma; "Nonlinear optical susceptibility of  $\text{Fe}_2\text{O}_3$  thin film synthesized by a modified sol-gel method", *J Sol-Gel.Sci.Technol.*, **19**, 539 (2000).
- [13] X.Gou, G.Wang, J.Park, H.Liu, J.Yang; "Monodisperse hematite porous nanospheres: synthesis, characterization, and application for gas sensors", *Nanotechnology*, **19**, 125606 (2008).
- [14] J.Zhang, X.Liu, L.Wang, T.Yang, X.Guo, S.Wu, S.Wang, S.Zhang; "Synthesis and gas sensing properties of  $\alpha\text{-Fe}_2\text{O}_3$  & ZnO core-shell nanospindles", *Nanotechnology*, **22**, 185501 (2011).
- [15] A.M.Redon, J.Vigneron, R.Heindl, C.Sella, C.Martin, J.P.Dalbera; Differences in the optical and photoelectrochemical behaviours of single-crystal and amorphous ferric oxide, *Sol.Cells*, **3**, 179 (1981).
- [16] J.S.Curran, W.Gissler; Different photoelectron chemical behavior of sintered and flame-oxidized  $\text{Fe}_2\text{O}_3$ , *J.Electrochem.Soc.*, **126**, 56 (1979).
- [17] A.Duret, M.Gratzel; Visible light-induced water oxidation on mesoscopic  $\alpha\text{-Fe}_2\text{O}_3$  films made by ultrasonic spray pyrolysis, *J.Phys.Chem.B*, **109**, 17184 (2005).
- [18] I.Cesar, A.Kay, J.A.Gonzalez Martinez, M.Gratzel; Translucent thin film  $\text{Fe}_2\text{O}_3$  photoanodes for efficient water splitting by sunlight: nanostructure-directing effect of Si-doping, *J.Am.Chem.Soc.*, **128**, 4582 (2006).
- [19] A.Kay, I.Cesar, M.Gratzel; New benchmark for photooxidation by nanostructured  $\alpha\text{-Fe}_2\text{O}_3$  films, *J.Am.Chem.Soc.*, **128**, 15714 (2006).
- [20] J.A.Glasscock, P.R.F.Barnes, I.C.Plumb, N.Savvides; Enhancement of photoelectrochemical hydrogen production from hematite thin films by the introduction of Ti and Si, *J.Phys.Chem.C*, **111**, 16477 (2007).
- [21] H.Miyake, H.Kozuka; Photoelectrochemical properties of  $\text{Fe}_2\text{O}_3\text{-Nb}_2\text{O}_5$  films prepared by sol-gel method, *J.Phys.Chem. B*, **109**, 17951 (2005).
- [22] H.E.Prakasam, O.K.Varghese, M.Paulose, G.K.Mor, C.A.Grimes; Synthesis and photoelectrochemical properties of nanoporous iron (III) oxide by potentiostatic anodization, *Nanotechnology*, **17**, 4285 (2006).
- [23] H.L.Sanchez, H.Steinfink, H.S.White; Solid solubility of Ge, Si and Mg in  $\text{Fe}_2\text{O}_3$  and photoelectric behavior, *J.Solid State Chem.*, **41**, 90 (1982).
- [24] R.K.Quinn, R.D.Nasby, R.J.Baughman; Photoassisted electrolysis of water using single-crystal  $\alpha\text{-Fe}_2\text{O}_3$  anodes, *Mater.Res.Bull.*, **11**, 1011 (1976).
- [25] C.Sanchez, K.D.Sieber, G.A.Somorjai; The photoelectrochemistry of niobium doped  $\alpha\text{-Fe}_2\text{O}_3$ , *J. Electroanal. Chem.*, **252**, 269 (1988).
- [26] S.Li and G.Rusu; *J.Optoelectron.Adv.Materials*, **7**, 817 (2005).
- [27] J.I.Pankove; *Optical processes in semiconductors*, Dover Publications Inc., New York, 91 (1975).
- [28] F.Yakuphanoglu, A.Cukurovali, I.Yilmaz; *Opt.Mater.*, **27**, 1366 (2005).

**Full Paper**

---

- [29] F.Urbach; Phys.Rev., **92**, 1324 (1953).
- [30] M.Didomenico, S.H.Wemple, J.Appl.Phys., **40**, 720 (1969).
- [31] S.H. Wemple, M.Didomenico; Phys.Rev.B, **3**, 1338 (1971).
- [32] S.Adachi; Optical properties of crystalline and amorphous semiconductors: materials and fundamental principles, Kluwer Academic, Boston, (1999).
- [33] M.DiDomenico, S.H. Wemple; J.Appl.Phys., **40**, 720 (1969).
- [34] M.Modreanu, M.Gartner, N.Tomozeiu; J.Seekamp, P.Cosmin, Opt.Mater., **17**, 145 (2001).
- [35] A.K.Wolaton, T.S.Moss; Proc.Roy.Soc., **81**, 5091 (1963).
- [36] F.Yakuphanoglu, A.Cukurovali, I.Yilmaz; "Determination and analysis of the dispersive optical constants of some organic thin films", Phys.B: Condensed Matt., **351**,53 (2004).